Dynamics of an exclusion process with creation and annihilation

2004 J. Phys. A: Math. Gen. 37 3933

(http://iopscience.iop.org/0305-4470/37/13/002)

INSTITUTE OF PHYSICS PUBLISHING JOURNAL OF PHYSICS A: MATHEMATICAL AND GENERAL

J. Phys. A: Math. Gen. **37** (2004) 3933–3944 PII: S0305-4470(04)72430-0

Dynamics of an exclusion process with creation and annihilation

Róbert Juhász and Ludger Santen

Theoretische Physik, Universität des Saarlandes, 66041 Saarbrücken, Germany

E-mail: juhasz@lusi.uni-sb.de and santen@lusi.uni-sb.de

Received 12 November 2003, in final form 17 February 2004
Published 17 March 2004
Online at stacks.iop.org/JPhysA/37/3933 (DOI: 10.1088/0305-4470/37/13/002)

Abstract

We examine the dynamical properties of an exclusion process with creation and annihilation of particles in the framework of a phenomenological domain-wall theory, by scaling arguments and by numerical simulation. We find that the length and the time scales are finite in the maximum current phase for finite creation and annihilation rates as opposed to the algebraically decaying correlations of the totally asymmetric simple exclusion process (TASEP). Critical exponents of the transition to the TASEP are determined. The case where bulk creation and annihilation rates vanish faster than the inverse of the system size N is also analysed. We point out that shock localization is possible even for rates proportional to N^{-a}, $1 < a < 2$.

PACS numbers: 05.60.−k, 87.16.Uv, 87.16.Nn, 05.70.Ln

1. Introduction

Self-driven many-particle systems have been extensively investigated in recent years. The ongoing research interest in this kind of systems is both conceptual [1–5] and motivated by many important applications in different fields [6–13]. Stochastic models of self-driven many-particle systems have been used in order to describe vehicular transport [6, 7], pedestrian dynamics [7], intracellular transport [8–10] and many other problems [11–13]. The common feature of these models is the steady input of energy, which leads to generic non-equilibrium behaviour [13]. This feature implies that the standard methods applied in equilibrium statistical mechanics have to be generalized in order to handle such systems. First steps in this direction have been made: exact solutions of the stationary state have been obtained [14, 15], a quantum formalism was established, which rewrites the master equation as a Schrödinger equation in imaginary time [1], Yang–Lee zeros have been introduced in order to describe non-equilibrium phase transition [4] and for a number of transport models a free-energy formalism has been developed [3].

A question, which naturally arises, is how the properties of such systems are influenced by the presence or absence of conserved quantities. This issue has been studied by the example of the totally asymmetric simple exclusion process (TASEP) [16, 17], which is the most simple non-trivial driven many-particle model. TASEP with particle reservoir which allow for particle exchange in the bulk was essentially introduced by Willmann *et al* as a model of a limit order market [18]. In this paper we study this model in the form as defined by Parmeggiani *et al* [19] therefore we refer to it as PFF model in the following. This model can be viewed in the above sense as the grand-canonical counterpart of the TASEP and was motivated by the motion of molecular motors, which move along one-dimensional filaments [8–11]. It describes correctly the stochastic and biased motion of particles, the discrete structure of the filaments as well as the finite length of the path between attachment and detachment of a motor, which can be tuned by adapting the capacity of the bulk reservoir. If one considers the PFF model with open boundaries the particle exchange in the bulk may lead to the localization of an interface separating a high- and a low-density domain in the bulk. In addition to this, the structure of the phase diagram differs strongly from that of the TASEP with particle conservation [19–23]. In the present work, we investigate the dynamical properties of this model by phenomenological and numerical methods.

The paper is organized as follows. In the next section, the model is re-introduced and the most important features of its stationary state are reviewed. In section 3, we examine the dynamical properties of the model in the shock phase by means of studying the density–density autocorrelation function which we relate to a phenomenological theory of domain-wall motion. The phase diagram of the model is given in the case of vanishing total capacity of the bulk reservoir. Phenomenological results are then compared to direct simulations of the model. In section 4, we discuss the length and time scales in the maximum current phase by means of scaling arguments and numerical simulation. A summary and discussion of the results follow in the final section.

2. The model

The PFF model [18, 19] is defined on a one-dimensional lattice of N sites, each of which can either be empty ($\tau_i = 0$) or occupied by a single particle ($\tau_i = 1$). In the bulk of the system particles interact via asymmetric exclusion dynamics, i.e. particle on site i jumps to the neighbouring site $i + 1$ with rate 1 provided it is empty. Boundary sites are coupled to particle reservoirs, which realize in- and output rates, whereas bulk sites change particles with a bulk reservoir. To be concrete: particles enter the system randomly on site 1 with attempt rate α, and they can leave the Lth site with rate β. At bulk sites $1, 2, \ldots, L$ particles can attach with attempt rate ω_A and detach with rate ω_D.

The stationary density $\langle \tau_i \rangle$ and current profiles $\langle j_i \rangle = \langle \tau_i(1 - \tau_i) \rangle$ have been recently studied by a continuous mean field approximation [19–21]. The attachment and detachment rates were taken to be proportional to $1/N$, i.e. $\omega_A = \Omega_A/N$, $\omega_D = \Omega_D/N$, where Ω_A and Ω_D are constants, and the thermodynamical limit $N \to \infty$ was considered. The lattice constant was rescaled according to $b = 1/N$ so the spatial coordinate $x = i/N$ becomes a continuous variable in this limit. Neglecting the density–density correlations and the spatial derivatives higher than the first-order one, one obtains the following equation for the stationary density profile $\rho(x)$ [20]:

$$(1 - 2\rho)\frac{\partial \rho}{\partial x} - \Omega_D[K - (1 + K)\rho] = 0 \tag{1}$$

where $K = \omega_A/\omega_D$. The stationary density profile $\rho(x)$ can be constructed from the flow-field of (1). In order to adapt the solution of (1) to the boundary conditions one has to integrate (1)

from the left ($\rho(0) = \alpha$) and right boundary ($\rho(1) = 1 - \beta$), respectively. This leads to the following implicit expressions for the density profile [20]:

$$\begin{aligned} x &= \frac{1}{\Omega_D(1+K)}\frac{K-1}{(1+K)}\ln\left|\frac{K-(1+K)\rho_-}{K-(1+K)\alpha}\right| + \frac{2(\rho_- - \alpha)}{\Omega_D(1+K)} \\ 1-x &= \frac{1}{\Omega_D(1+K)}\frac{K-1}{(1+K)}\ln\left|\frac{K-(1+K)\overline{\beta}}{K-(1+K)\rho_+}\right| + \frac{2(\overline{\beta} - \rho_+)}{\Omega_D(1+K)} \end{aligned} \tag{2}$$

where $\overline{\beta} = 1 - \beta$ and ρ_- (ρ_+) denotes the solution of (1) obtained by integration from the left (right) boundary. The selection of the left or right solution is realized by means of characteristics, which determine the velocity of discontinuity of the density profile $\rho(x)$ [20]. If the velocity of this so-called shock is finite for any position in the bulk x, it is driven out of the system and the stationary density profile is continuous. In contrast to this, a localized shock is observed if

$$\rho_-(x_s) + \rho_+(x_s) = 1 \tag{3}$$

holds for a particular position $0 < x_s < 1$. The profiles constructed in the above way are believed to be exact in the $N \to \infty$ limit [20, 21].

In [20] it has also been pointed out that the leading finite-size corrections of the density profile in the shock regime can be obtained by applying the domain-wall theory for the dynamics of the shock, which was originally developed for the TASEP [24] and has been recently generalized to models without particle conservation [20, 21]. The idea of this approach is to describe the stochastic motion of the domain wall by a random walk with hopping rates determined by the particle current in the low- and high-density domains. In the case of the TASEP the hopping rates are constant, as the current is constant due to particle conservation. In contrast to this, for the PFF model one observes nontrivial current profiles $j(x)$, which lead to position-dependent hopping rates:

$$w_l(x) = \frac{j_-(x)}{\rho_+(x) - \rho_-(x)} \qquad w_r(x) = \frac{j_+(x)}{\rho_+(x) - \rho_-(x)} \tag{4}$$

where $\rho_\pm(x)$ and $j_\pm(x) = \rho_\pm(x)(1 - \rho_\pm(x))$ are the density and the current in the high(+) and low(−) density domain, respectively. The potential landscape governing the motion of the walker has a minimum at x_s, which we will refer to as the equilibrium shock position. Previous analysis of the TASEP has shown that the random walk picture for the domain-wall motion gives a correct description of time-dependent phenomena as well [26–29]. So we believe that this phenomenological description is appropriate also for the dynamical properties of the PFF model.

3. The shock phase

3.1. The case $\omega_{A,D} = \Omega_{A,D}/N$

In this section, we discuss the dynamical properties of the model for parameter combinations where the density profile has a discontinuity separating a high- and a low-density domain.

First we consider the case where the total 'capacity' of the bulk reservoir is comparable with that of the boundary reservoirs, i.e. $\omega_A = \Omega_A/N, \omega_D = \Omega_D/N$. The density profile of this model was thoroughly studied and the parameter regime where the system exhibits a shock is known (see the phase diagram in [20]).

In order to establish the relevant time scale, we consider the stationary (density–density) autocorrelation function $C(i,t) \equiv \langle \tau_i(0)\tau_i(t)\rangle$, where $\langle \cdots \rangle$ denotes the average over the

stationary ensemble. One expects that the dominant dynamical mode in a finite system, which determines the long time behaviour of temporal correlations in the vicinity of the equilibrium shock position x_s, is the stochastic motion of the domain wall as opposed to 'microscopic' processes. Thus, for large N the local density at a given time t is appropriately described by the function

$$\tau(x,t) = \rho_+(x) + (\rho_-(x) - \rho_+(x))\theta(\xi(t) - x) \tag{5}$$

where $\theta(x)$ is the Heaviside function and $\xi(t)$ is a random walk with steps of length $1/N$ and with hopping rates given in (4). The potential well which the walker is trapped in is well approximated by a harmonic potential in the vicinity of its minimum x_s. Considering the continuous description of the random walk the Fokker–Planck equation reads [32]

$$\frac{\partial P}{\partial t} = \frac{V}{N}\frac{\partial}{\partial y} y P(y,t) + \frac{D}{N^2}\frac{\partial^2 P}{\partial y^2} \tag{6}$$

where $y = x - x_s$ is the deviation from the equilibrium shock position. The constants V and D, which characterize the shape of the potential, are given by

$$\begin{aligned} V &\equiv \frac{\mathrm{d}w_l(x_s)}{\mathrm{d}x} - \frac{\mathrm{d}w_r(x_s)}{\mathrm{d}x} \\ D &\equiv w_l(x_s) = w_r(x_s). \end{aligned} \tag{7}$$

For the PFF model we have $V = \Omega_A + \Omega_D$. Equation (6) is the Fokker–Planck equation of the Ornstein–Uhlenbeck process [32], and has the time-dependent solution:

$$\begin{aligned} P(y,t) &\equiv P(y,t|y_0,0) \\ &= \left[\frac{2\pi D}{N^2(\omega_A+\omega_D)}(1 - \mathrm{e}^{-2(\omega_A+\omega_D)t})\right]^{-1/2} \\ &\quad \times \exp\left[-\frac{N^2(\omega_A+\omega_D)}{2D}\frac{(y - y_0\,\mathrm{e}^{-(\omega_A+\omega_D)t})^2}{1 - \mathrm{e}^{-2(\omega_A+\omega_D)t}}\right]. \end{aligned} \tag{8}$$

For large system sizes the harmonic approximation is expected to give an appropriate description of the shock dynamics, since the localization length of the walker increases only sub-extensively ($\sim N^{1/2}$).

In the framework of the above phenomenological picture the autocorrelation function is given by

$$\begin{aligned} C(y,t) &\equiv \langle \tau(y,0)\tau(y,t)\rangle \\ &= \rho_-(y)[2\rho(y) - \rho_-(y)] + [\rho_+(y) - \rho_-(y)]^2 I(y,t) \end{aligned} \tag{9}$$

where

$$\begin{aligned} I(y,t) &\equiv \langle \theta(\xi(t) - y)\theta(\xi(0) - y)\rangle \\ &= \int_{-x_s}^{y} \mathrm{d}x_0 \int_{-x_s}^{y} \mathrm{d}x\, P(x + x_s, t|x_0 + x_s, 0) P_{st}(x_0 + x_s). \end{aligned} \tag{10}$$

Inserting now (8) into (10) we obtain

$$\begin{aligned} I(y,t) = \sqrt{\frac{N^2(\omega_A+\omega_D)}{8\pi D}} \int_{-\infty}^{0} \mathrm{e}^{-\frac{N^2(\omega_A+\omega_D)}{2D}(x+y)^2} \\ \times \operatorname{erfc}\left(\sqrt{\frac{N^2(\omega_A+\omega_D)}{2D(1-T^2)}}(T(x+y) - y)\right)\mathrm{d}x, \end{aligned} \tag{11}$$

where $T = \mathrm{e}^{-(\omega_A+\omega_D)t}$ and $\operatorname{erfc}(x)$ is the complementary error function.

The integral $I(y,t)$ can be evaluated only at the equilibrium position of the shock, i.e. for $y=0$, where we obtain the well-known result

$$I(0,t)=\frac{1}{4}+\frac{1}{2\pi}\arcsin[\mathrm{e}^{-(\omega_A+\omega_D)t}]. \tag{12}$$

For $y\neq 0$, $I(y,t)$ cannot be calculated analytically, however, it can be expanded for short ($(\omega_A+\omega_D)t\ll 1$) and long times ($(\omega_A+\omega_D)t\gg 1$). In the latter case the asymptotic form of $I(y,t)$ is given by

$$I(y,t)=\frac{1}{4}\left(1+\operatorname{erf}\left[y\sqrt{\frac{N^2(\omega_A+\omega_D)}{2D}}\right]\right)^2 + \frac{1}{2\pi}\,\mathrm{e}^{-\frac{N^2(\omega_A+\omega_D)}{D}y^2}\,\mathrm{e}^{-(\omega_A+\omega_D)t}+\mathcal{O}(\mathrm{e}^{-2(\omega_A+\omega_D)t}). \tag{13}$$

This expression shows that the motion of the domain wall introduces a time scale $\tau=\frac{1}{\omega_A+\omega_D}=\frac{N}{\Omega_A+\Omega_D}$, which is proportional to the system size. Note that this time scale τ is independent of the position y. However, the domain-wall contribution to the true correlation function is relevant only in the region $|y|\ll N^{-1/2}$ and its amplitude is exponentially suppressed when leaving the equilibrium shock position.

It is also interesting to discuss the short time behaviour of $I(y,t)$, i.e the case $(\omega_A+\omega_D)t\ll 1$. Here, the expansion of (11) yields

$$I(y,t)=\frac{1}{2}\left(1+\operatorname{erf}\left[y\sqrt{\frac{N^2(\omega_A+\omega_D)}{2D}}\right]\right)-\mathrm{e}^{-\frac{N^2(\omega_A+\omega_D)}{2D}y^2}\frac{1}{\pi}\sqrt{\frac{\omega_A+\omega_D}{2}}t^{1/2}+\cdots. \tag{14}$$

The leading order correction is thus proportional to $t^{1/2}$. This is analogous to the TASEP with parallel dynamics, where the space- and time-dependent correlation functions are exactly known [25]. This asymptotic form corresponds to a $f^{-3/2}$ power spectrum of the local density fluctuations as it was found in the case of the TASEP [26].

3.2. The case of vanishing total capacity of the bulk reservoir

We now turn to discuss the case where ω_A and ω_D vanish faster than $1/N$. In [19, 21] it was then argued that the effect of bulk reservoir is negligible in the thermodynamic limit, and the system will behave as the TASEP. We have found that this scenario is correct for any parameter combination *except* the line $\alpha=\beta<1/2$. Consider at this particular line the general case where attach and detach rates scale as $\omega_{A,D}=\Omega_{A,D}/N^a$. We claim that a shock in the density profile is still observed in the thermodynamic limit whenever $1\leqslant a<2$. Substituting $\omega_{A,D}=\Omega_{A,D}/N^a$ into the calculations of the previous subsection one obtains that the width of the shock grows with the system size as $\xi=N\Delta x\sim N^{\frac{a}{2}}$, whereas the time scale as $\tau\sim N^a$. Therefore, as long as $1\leqslant a<2$, the localization length of the domain wall increases only sub-extensively, and an unbounded motion (as for the TASEP with $\alpha=\beta<1/2$), is only observed if $a>2$. This is also true for the related time scale τ. The time scale in the TASEP is known to diverge proportionally to N^2 [26, 27, 29]. Therefore if $1\leqslant a<2$ the time scale is determined by the attach and detach processes ($\tau\sim N^a$), while TASEP-like behaviour ($\tau\sim N^2$) is observed only if $a\geqslant 2$.

In the case $1<a<2$ the average density takes the values α in the low-density domain and $1-\alpha$ in the high-density domain if $N\to\infty$. Thus, the location of the discontinuity in the $N\to\infty$ limit can be obtained by substituting $\rho_-(x)=\text{const}=\alpha$ and $\rho_+(x)=\text{const}=1-\alpha$ into (1). Equation (3) then yields

$$x_s=\frac{1-\alpha(1+K)}{(1+K)(1-2\alpha)}. \tag{15}$$

Note that x_s is independent of a. Thus, a shock can be found in the system, whenever

$$\frac{\alpha}{1-\alpha} < K < \frac{1-\alpha}{\alpha}.$$

If $\frac{\alpha}{1-\alpha} > K$ $\left(K > \frac{1-\alpha}{\alpha}\right)$ the system is in the low-(high)-density phase.

For $\alpha \neq \beta$ and $a > 1$ it is not possible to balance the current in the low- and high-density domains, i.e. to fulfil relation (3) for any $0 < x < 1$ in the $N \to \infty$ limit. Hence the shock is driven out of the system and the density profile of the TASEP is recovered.

The description of the domain-wall dynamics by a random walk implies that the dynamical exponent (defined as $\tau \sim \xi^z$) is $z = 2$. The same exponent can be observed for the TASEP at the transition line $\alpha = \beta < 1/2$, where the length and time scales are infinite in the limit $N \to \infty$, whereas for finite systems they scale as $\xi \sim N$ and $\tau \sim N^2$, i.e. $z = 2$. In the case of the TASEP this divergence is restricted to the transition line $\alpha = \beta < 1/2$, because the domain-wall motion is biased if $\alpha \neq \beta$. In the case of the PFF model the position-dependent hopping rates introduce a localization length which grows sub-extensively in the whole shock phase. Here, the transition between shock- and low-density phases or shock- and high-density phases is not a localization–delocalization transition, but it simply means that the equilibrium shock position moves to the system boundaries. At the transition line the random walker is trapped in a potential with hard-core repulsion for $y < 0$ (HD-S transition) or $y > 0$ (LD-S transition) respectively. The complementary part of the potential landscape can still be described by the harmonic approximation.

Finally, we mention that the domain-wall contribution of the connected autocorrelation function $C_{\mathrm{conn}}(y, t, N) \equiv \langle \tau(y,0)\tau(y,t)\rangle - \langle \tau(y,0)\rangle^2$ has the following scaling form:

$$C_{\mathrm{conn}}(y, t, N) = \tilde{C}(y^2 N^{2-a}, t N^{-a}).$$

We stress that the contribution to the long time behaviour of the autocorrelation function, induced by the domain-wall movement is relevant in a finite system only at sites $|y| \ll N^{\frac{a}{2}-1}$.

3.3. Numerical results

In this subsection, we compare the phenomenological results obtained in the previous parts of this section with results of direct numerical simulation of the model. In the numerical investigations we have mainly considered the case $a = 1, \Omega_A = \Omega_D \equiv \Omega$, where the equilibrium position of the shock x_s and the diffusion constant D can be explicitly given. Equation (1) can be solved for $\rho_+(x)$ and $\rho_-(x)$ and condition (3) yields $x_s = \frac{\beta-\alpha}{2\Omega} + \frac{1}{2}$. The diffusion constant is given by $D = \frac{1}{4}(1/\Delta - \Delta)$ where $\Delta = 1 - \alpha - \beta - \Omega$ is the height of the shock [20].

The connected autocorrelation function was computed for system sizes $N = 201$–2001. Results at the equilibrium position of the shock ($y = 0$) are shown in figures 1 and 2. As can be seen in the figures the phenomenological predictions are in good agreement with the numerical results except for short times, and the accuracy of the phenomenological description improves for larger system sizes, as was found in the case of the stationary density profile [20]. A rapid decay of the autocorrelation function can be observed on a time scale $t \sim \mathcal{O}(1)$, which is connected to the 'self-correlation' of particles, i.e. the contribution of the particles which are not updated during time t. This 'microscopic' time scale is related to the particle current and can be identified as the finite time scale in the high- and low-density domains of the TASEP [27, 29]. The above phenomenological picture apparently does not account for this contribution, nevertheless the crossover to the regime, which is dominated by the motion of the domain wall, takes place at rather short times of $\mathcal{O}(1/N)$.

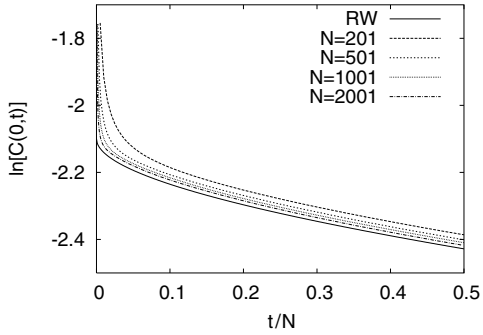

Figure 1. The connected autocorrelation function measured at $y = 0$ for different system sizes and with parameters $\alpha = 0.1$, $\beta = 0.1$ and $\Omega = 0.1$. The solid line is the phenomenological prediction given by (9) and (12).

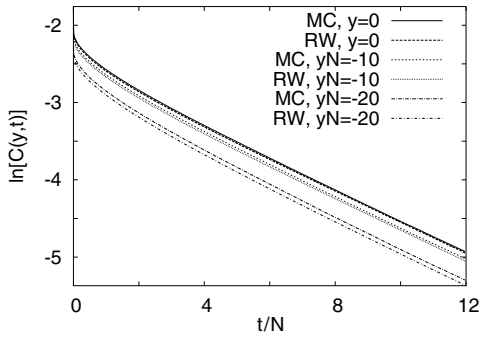

Figure 2. The connected autocorrelation function measured at different positions in the chain for system size $N = 1001$ and with parameters as in figure 1. The phenomenological curve for $y \neq 0$ was obtained by integrating (11) numerically.

In figure 2 results for sites away from the equilibrium shock position ($y \neq 0$) are presented. The accuracy of the phenomenological theory is less satisfying as sites leave the equilibrium shock position. This discrepancy, which increases with larger distances from the equilibrium shock position, may be related to the anharmonicity of the potential well.

4. Maximum current phase

The existence of a maximum current phase in the presence of bulk particle exchange is restricted to the case $\omega_A = \omega_D \equiv \omega$ (see [20]). Furthermore, we assume that the rate ω does not scale with the system size, i.e. $a = 0$. Compared to the maximal current phase of the TASEP we expect that temporal correlations are reduced, as the typical lifetime of particles is finite, and this may introduce a finite time scale. This was also observed in [18] where the correlation function and fluctuations of price increments were investigated and the corresponding time scale was found to be ω^{-1}. Here, we study the connected density–density autocorrelation function at the site in the middle of the chain. Since the validity of the phenomenological treatment presented above is restricted to the shock phase, we resort to scaling arguments and numerical simulations. To our knowledge, this correlation function has not yet been investigated in the maximum current phase even in the case of particle conservation in the bulk. Therefore, we examine the dynamical correlations in the TASEP first.

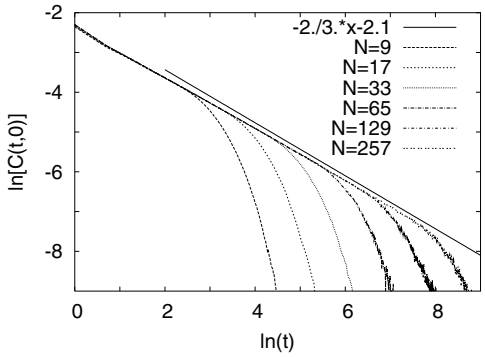

Figure 3. The connected autocorrelation function in the maximum current phase ($\alpha = \beta = 0.5$) of the TASEP ($\omega_A = \omega_D = 0$) for different system sizes.

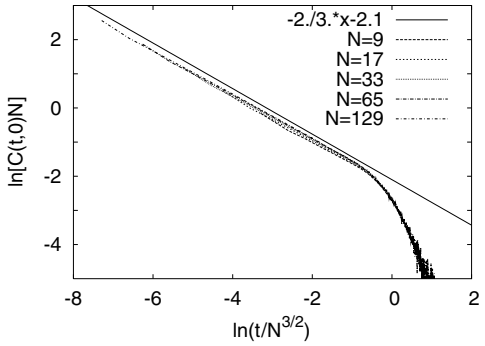

Figure 4. The scaled connected autocorrelation function in the maximum current phase ($\alpha = \beta = 0.5$) of the TASEP ($\omega_A = \omega_D = 0$).

Let us assume that the connected autocorrelation function is a homogeneous function of its variables N and t. Rescaling then the lengths by a factor b it transforms as

$$C(N,t) = b^{-x}\tilde{C}(N/b, t/b^{3/2}) \qquad \omega = 0 \tag{16}$$

where we have used that the dynamical exponent is $z = 3/2$ in the maximum current phase [29, 30]. The scaling dimension x can be guessed as follows. The fluctuations of the total particle number scale with the system size as $\sim N^{1/2}$ [33, 34]. As a consequence the fluctuations of the local density scale as $\sim N^{-1/2}$. Since the autocorrelation function contains a product of two local density operators, we have $x = 1$. Setting now $t = b^{3/2}$ in (16) and taking the limit $N \to \infty$ we obtain $C(t) \sim t^{-2/3}$, whereas choosing $b = N$ we get

$$C(N,t) = N^{-1}\Phi(t/N^{3/2}) \tag{17}$$

where the scaling function $\Phi(x)$ behaves as

$$\begin{aligned} &\Phi(x) \sim x^{-2/3} \qquad && x \ll 1 \\ &\Phi(x) \sim 0 && x \gg 1. \end{aligned} \tag{18}$$

Numerical results for the autocorrelation function are shown in figure 3, indicating an algebraic decay with an exponent compatible with $2/3$, and the scaling plot in figure 4 is in accordance with (17).

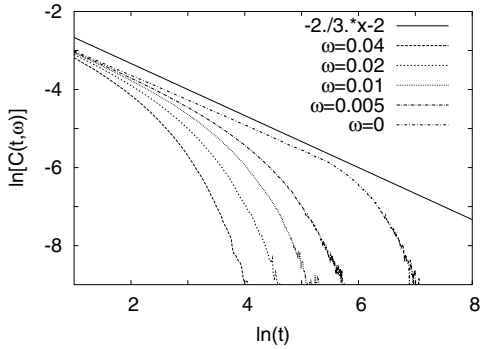

Figure 5. The connected autocorrelation function in the maximum current phase ($\alpha = \beta = 0.5$) for different rates ω. The size of the system is $N = 257$.

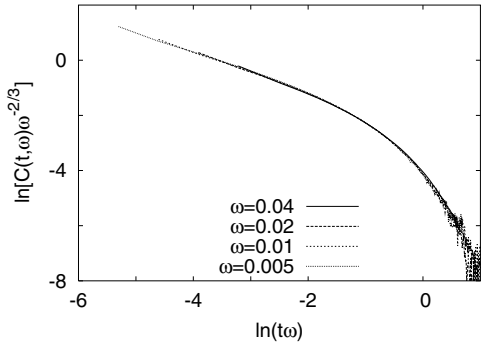

Figure 6. Scaling plot of the connected autocorrelation function in the maximum current phase ($\alpha = \beta = 0.5$) according to (20).

For finite ω and infinite system size one expects the following behaviour of the autocorrelation function when time is rescaled by a factor b:

$$C(t, \omega) = b^{-2/3}\overline{C}(t/b, \omega b) \qquad 1/N = 0. \tag{19}$$

Setting $b = 1/\omega$ we have

$$C(t, \omega) = \omega^{2/3}\Psi(t\omega) \qquad 1/N = 0 \tag{20}$$

where the scaling function $\Psi(x)$ behaves as $\Phi(x)$. Numerical results for finite ω are shown in figures 5 and 6. These are in agreement with (20), showing a cut-off at a time scale $\tau \sim \omega^{-1}$ which is the typical lifetime of particles [18].

Next, we determine the length scale ξ in the infinite system. In order to establish ξ we have studied the asymptotical decay of the density profile. For the TASEP the density profile is known to approach its bulk value $1/2$ algebraically [15, 17]. In contrast to this, the particle creation and annihilation processes lead to an exponentially fast asymptotical approach to the bulk density. To see this, consider the second-order mean field equation for the stationary density profile [19]

$$\frac{1}{2N}\frac{\partial^2\rho}{\partial x^2} + (2\rho - 1)\left(\frac{\partial\rho}{\partial x} - N\omega\right) = 0. \tag{21}$$

The solution of (21) in the asymptotic region where $\rho(x) - \frac{1}{2} \ll 1$, has the form $\rho(x) - \frac{1}{2} \sim \mathrm{e}^{-Nx/\xi_{mf}}$. Putting this into (21) yields $\xi_{mf} = \frac{1}{2\sqrt{\omega}}$. The scale of the decay

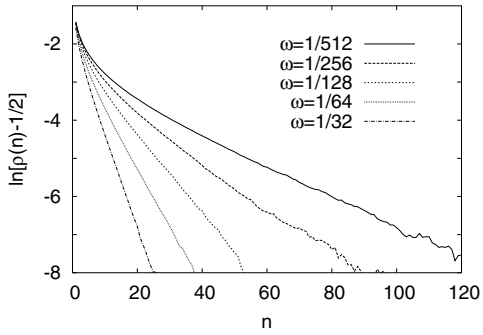

Figure 7. Density profile in the maximum current phase ($\alpha = \beta = 1$) for different rates ω. The size of the system is $N = 512$.

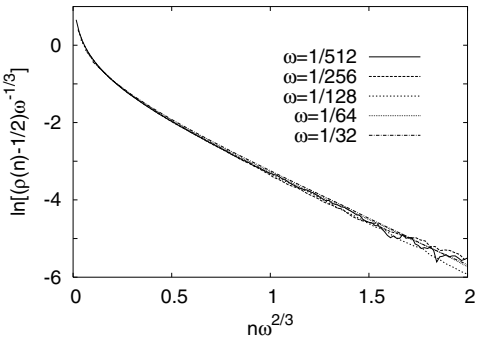

Figure 8. Scaling plot of the density profile in the maximum current phase ($\alpha = \beta = 1$). The size of the system is $N = 512$.

ξ_{mf} can then be identified as a finite length scale of the system. However, the true behaviour of ξ is not recovered by the mean field approximation as we show below.

Considering ω as a control parameter, the point $\omega = 0$ (TASEP) can be regarded as a critical point of the PFF model, where length and time scales diverge. We expect that in the vicinity of the critical point, i.e. for the PFF model with $\omega \ll 1$ the dynamical exponent is the same as strictly at criticality, i.e. that $\tau \sim \xi^{3/2}$ holds. Comparing this with $\tau \sim \omega^{-1}$ we obtain

$$\xi \sim \omega^{-\nu} \qquad \nu = 2/3. \tag{22}$$

In this context the exponent ν plays the role of the correlation length exponent. The correctness of (22) is supported by numerical results for the density profile shown in figures 7 and 8.

Thus, we have seen that the length and the time scales remain finite in the thermodynamic limit as long as ω does not vanish in that limit, i.e. $a = 0$. If $a > 0$, apparently both the length and the time scales diverge in the $N \to \infty$ limit, as in the case of the TASEP. However, for $a < \frac{3}{2}$ they scale with exponents that are different from those of the TASEP, namely $\xi \sim N^{\frac{2}{3}c}$, $\tau \sim N^{c}$, where $c = \min\{a, \frac{3}{2}\}$.

5. Discussion

The analysis of the dynamical properties completes the description of the stationary state of the PFF model. In the framework of a phenomenological domain-wall theory we could establish

a time scale in the vicinity of the equilibrium domain-wall position, which grows with the system size as $\sim N^a$. The localization length of the domain wall scales as $\sim N^{\frac{a}{2}}$, leading to the dynamical exponent $z = 2$, which is identical to that of the TASEP at the coexistence line $\alpha = \beta$. This is in both cases the consequence of the diffusive nature of the dominant dynamical mode. However, in the PFF model it is relevant only in a sub-extensively growing region whereas in the latter one in the whole system. Apart from the shock region the time scale is finite, and is related to the inverse of the particle current. In contrast to the TASEP the current is position dependent, a feature of the model which is reflected by the position dependence of the time scale. This position-dependent microscopic time scale is observed in the high- and low-density phases, as well. We note that the transition from the shock- to high-density (or low-density) phase manifests itself simply in the equilibrium domain-wall position leaving the system and it is not a delocalization transition as in the case of the TASEP. We have pointed out that for $\alpha = \beta < 1/2$ even a vanishing total capacity of the bulk reservoir ($1 < a < 2$) is able to localize the shock. We mention that the phenomenological calculations presented in this work can be carried out for arbitrary systems possessing a localized fluctuating domain wall, such as the model recently introduced by Rákos *et al* [35].

In the maximum current phase of the TASEP we have found the algebraic decay of the autocorrelation function. By scaling arguments we could determine the decay exponent which was found to be $2/3$. The introduction of noise through bulk particle exchange with a finite rate destroys the power-law correlations and the resulting phase is characterized by finite length and time scales. Thus, the TASEP can be regarded as a critical point of the PFF model. By scaling arguments we have determined the critical exponents which are in accordance with the results of numerical simulations.

Acknowledgments

We thank F Iglói and J Krug for useful discussions. This work has been supported by the Deutsche Forschungsgemeinschaft under grant no SA864/2-1.

References

[1] Schütz G M 2001 *Phase Transitions and Critical Phenomena* vol 19 ed C Domb and J L Lebowitz (San Diego: Academic)
[2] Evans M R and Blythe R A 2002 *Physica* A **313** 110
[3] Derrida B and Lebowitz J L 1998 *Phys. Rev. Lett.* **80** 209
[4] Arndt P F 2000 *Phys. Rev. Lett.* **84** 814
[5] Hinrichsen H 2000 *Adv. Phys.* **49** 815
[6] Chowdury D, Santen L and Schadschneider A 2000 *Phys. Rep.* **329** 199
[7] Helbing D 2001 *Rev. Mod. Phys.* **73** 1067
[8] Jülicher F, Ajdari A and Prost J 1997 *Rev. Mod. Phys.* **69** 1269
[9] Howard J 2001 *Mechanics of Motor Proteins and the Cytoskeleton* (Sunderland: Sinauer)
[10] Howard J 1997 *Nature* **389** 561
[11] Alberts B, Bray D and Lewis J 1994 *Molecular Biology of the Cell* (New York: Garland)
[12] Flyvbjerg H, Jülicher F, Ormos P and David F (ed) 2002 *Physics of Bio-Molecules and Cells* (Heidelberg: Springer)
[13] Privman V (ed) 1997 *Nonequilibrium Statistical Mechanics in One Dimension* (Cambridge: Cambridge University Press)
[14] Derrida B, Evans M R, Hakim V and Pasquier V 1993 *J. Phys. A: Math. Gen.* **26** 1493
[15] Schütz G and Domany E 1993 *J. Stat. Phys.* **72** 277
[16] MacDonald J T and Gibbs J H 1969 *Biopolymers* **7** 707
[17] Krug J 1991 *Phys. Rev. Lett.* **67** 1882
[18] Willmann R D, Schütz G M and Challet D 2002 *Physica* A **316** 430

[19] Parmeggiani A, Franosch T and Frey E 2003 *Phys. Rev. Lett.* **90** 086601
[20] Evans M R, Juhász R and Santen L 2003 *Phys. Rev.* E **68** 026117
[21] Popkov V, Rákos A, Willmann R D, Kolomeisky A B and Schütz G M 2003 *Phys. Rev.* E **67** 066117
[22] Lipowsky R, Klumpp S and Nieuwenhuizen T M 2001 *Phys. Rev. Lett.* **87** 108101
[23] Klumpp S and Lipowsky R 2003 *J. Stat. Phys.* **113** 233
[24] Kolomeisky A, Schütz G M, Kolomeisky E B and Straley J P 1998 *J. Phys. A: Math. Gen.* **31** 6911
[25] Schütz G M 1993 *Phys. Rev.* E **47** 4265
[26] Takesue S, Mitsudo T and Hayakawa H 2003 *Phys. Rev.* E **68** 015103
[27] Dudzinski M and Schütz G M 2000 *J. Phys. A: Math. Gen.* **33** 8351
[28] Santen L and Appert C 2002 *J. Stat. Phys.* **106** 187
[29] Nagy Z, Appert C and Santen L 2002 *J. Stat. Phys.* **109** 623
[30] Gwa L H and Spohn H 1992 *Phys. Rev.* A **46** 844
[31] Bilstein U and Wehefritz B 1997 *J. Phys. A: Math. Gen.* **30** 4925
[32] van Kampen N G 1981 *Stochastic Processes in Physics and Chemistry* (Amsterdam: North-Holland)
[33] Derrida B and Evans M R 1993 *J. Physique* I **3** 311
[34] Meakin P, Ramanlal P, Sander L M and Ball R C 1986 *Phys. Rev.* A **34** 5091
[35] Rákos A, Paessens M and Schütz G M 2003 *Preprint* cond-mat/0305136